ARL-TR-9924 ● JUNE 2024

Air Blast Characterization: Impulse to Power

by Kevin L McNesby, Steven W Dean, and Dakota G Scott

NOTICES

Disclaimers

The findings in this report are not to be construed as an official Department of the Army position unless so designated by other authorized documents.

Citation of manufacturer's or trade names does not constitute an official endorsement or approval of the use thereof.

Destroy this report when it is no longer needed. Do not return it to the originator.

ARL-TR-9924 ● JUNE 2024

Air Blast Characterization: Impulse to Power

Kevin L McNesby, Steven W Dean, and Dakota G Scott
DEVCOM Army Research Laboratory

REPORT DOCUMENTATION PAGE

1. REPORT DATE	2. REPORT TYPE	3. DATES COVERED	
		START DATE	END DATE
June 2024	Technical Report	1 October 2023	1 May 2024

4. TITLE AND SUBTITLE
Air Blast Characterization: Impulse to Power

5a. CONTRACT NUMBER	5b. GRANT NUMBER	5c. PROGRAM ELEMENT NUMBER
5d. PROJECT NUMBER	**5e. TASK NUMBER**	**5f. WORK UNIT NUMBER**

6. AUTHOR(S)
Kevin L McNesby, Steven W Dean, and Dakota G Scott

7. PERFORMING ORGANIZATION NAME(S) AND ADDRESS(ES)	8. PERFORMING ORGANIZATION REPORT NUMBER
DEVCOM Army Research Laboratory ATTN: FCDD-RLA-WA Aberdeen Proving Ground, MD 21005	ARL-TR-9924

9. SPONSORING/MONITORING AGENCY NAME(S) AND ADDRESS(ES)	10. SPONSOR/MONITOR'S ACRONYM(S)	11. SPONSOR/MONITOR'S REPORT NUMBER(S)

12. DISTRIBUTION/AVAILABILITY STATEMENT
DISTRIBUTION STATEMENT A. Approved for public release: distribution unlimited.

13. SUPPLEMENTARY NOTES
ORCID(s): Dakota Scott, 0000-0002-5835-4384

14. ABSTRACT
Peak shock pressure (Pa) and positive phase duration (A-duration, s) reported by airborne blast pressure sensors are used to calculate the energy fluence (J/m^2) on target. This energy fluence is then divided by shock overpressure duration (s) to yield an average shock power (W/m^2) on target. A comparison is made to shock impulse (Pa*s) calculated using similar reported data. A link between power of the explosive that created the airborne shock and power measured at target is shown.

15. SUBJECT TERMS
Energy Sciences, Weapons Sciences, shock quantification, shock impulse, shock power, Friedlander equation, shock overpressure

16. SECURITY CLASSIFICATION OF:			17. LIMITATION OF ABSTRACT	18. NUMBER OF PAGES
a. REPORT	b. ABSTRACT	C. THIS PAGE		
UNCLASSIFIED	UNCLASSIFIED	UNCLASSIFIED	UU	29

19a. NAME OF RESPONSIBLE PERSON	19b. PHONE NUMBER *(Include area code)*
Kevin McNesby	(410) 306-1383

STANDARD FORM 298 (REV. 5/2020)
Prescribed by ANSI Std. Z39.18

Contents

List of Figures

Acknowledgments

The authors would like to thank Elliot Wainwright and Brian Barnes for useful discussions regarding this work.

1. Introduction

Measurement of peak shock overpressure and duration of shock overpressure have been studied for over 75 years.[1] Within the last several years, there has been increased emphasis[2] on quantifying airborne shock exposure (i.e., "blast") by military personnel during training. The injury accompanied by exposure to airborne shock is a complex type of physical trauma resulting from direct or indirect exposure to an explosion.[3] Quantifying the potential injury to personnel is difficult because the mechanism of injury is not fully understood, and measurement of shock peak pressures and durations is dependent on measurement gauge orientation and mounting, and distance from the center of mass of the explosion source.[4] Even for well-characterized airborne shocks, a single metric that can be correlated to severity of exposure does not exist. This work explores calculating power (watts) of an airborne shock using peak shock pressure and A-duration (time to first zero crossing of pressure after peak) reported by body-worn pressure sensors.

2. Reflected vs. Incident Shock

An explosively driven shock in air begins with a piston of some type (expanding detonation products, walls of a container enclosing explosives, etc.) rapidly pushing into air. If the piston is fast enough, the air molecules can "pile up" at the piston surface (Fig. 1A) and are accelerated to the velocity of the piston. When the piston slows (Fig. 1B), these piled-up accelerated air molecules are launched into ambient air and act as a new piston. This moving piled-up air piston collides with undisturbed air molecules, transferring momentum (mass × velocity) to the undisturbed molecules, creating a new piston of piled-up air molecules (Fig. 1C). This momentum transfer occurs continuously and creates what seems to be a moving piston of increased air density, but with the air molecules in the "piston" constantly changing. The net effect is a moving region of high-density air (the shock front) trailed by slower-moving air (the old air piston(s)). Because of the exchange of energy between the two, the velocity of the leading air piston is always decreasing, as is the velocity of air following the air piston. When the velocity of the leading air piston slows to the sound speed in air, the initial air shock has decayed to an acoustic wave.[5]

This qualitative discussion of a shock wave in air is meant to illustrate that an air shock consists of a narrow region of fast-moving, dense air molecules (the shock front) followed by a slower-moving, less dense (but above ambient) distribution of air molecules. As an example, an airborne shock front (air piston) moving near 400 m/s (with a thickness of <1 mm) will have a distribution of air molecules

following in its wake for approximately 25 mm. The shock front is responsible for the peak shock pressure. The air molecules following the shock front are responsible for most of the shock impulse[6] (product of pressure × time, Pa*s).

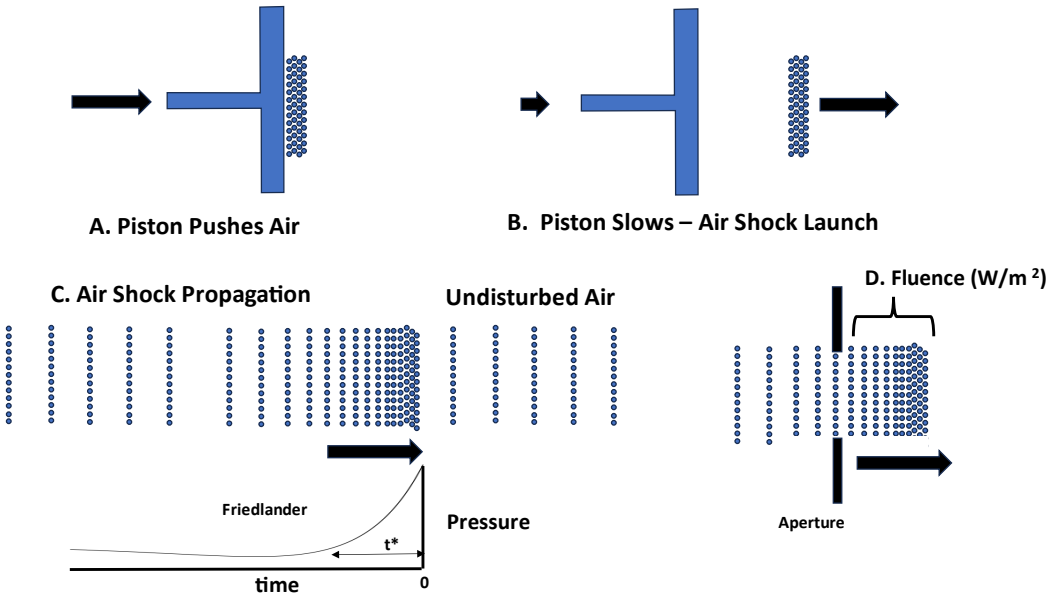

Fig. 1 A schematic showing A) the generation of an airborne shock from a piston moving air, B) airborne shock launch, C) air shock propagation, and D) passage of the shock through an aperture

When this moving ensemble of air molecules encounters a barrier, the force on that barrier is dependent on its orientation to the direction of motion of the moving air molecules. If the barrier is a solid surface or wall, with the plane of the surface normal to the direction of the moving air molecules, the air molecules hit the surface, slow to zero velocity, and then bounce away with their direction reversed. This occurrence is called reflected shock. Reflected shock deposits the most energy possible on the barrier.

If the barrier is a thin wall with its plane surface parallel to the direction of the shock, the air molecules can flow past the barrier. However, collisions between the shocked air molecules and undisturbed molecules in their path are not always on center, so some of the forward motion of the shocked air molecules causes motion at random angles to the initial air shock direction. These off-axis collisions create slower-moving air molecules that can now impact the plane of the barrier. However, because their velocity is a fraction of the initial shocked air molecules, the deposition of energy on the barrier is at a minimum. This occurrence is called incident shock. Incident shock deposits the least energy possible on the barrier.[7]

This explanation is important, because it shows how the energy that a shock deposits on a barrier is dependent on the orientation of that barrier to the direction

of the shock. This is manifested in the general measurement of shock pressures. If the barrier is now one surface of a capacitor (or piezoelectric crystal) exposed to shock, the deflection of that surface, and hence the voltage across the capacitor (or piezoelectric crystal), is highly dependent on the orientation to shock direction.[8,9]

As the shocked air (shock front and trailing air molecules) passes through an imaginary surface, the energy passing through the surface is called a flux, expressed as J/s/m^2 (the area is the area of the imaginary surface). The total energy that passes through the surface is called the fluence (J). A body-worn pressure gauge reports a pressure versus time record for an incoming airborne shock. This report documents the calculation of energy flux (W/m^2) based on data recorded by a body-worn gauge.

3. The Friedlander Equation

The time change of incident pressure as the airborne shock passes a fixed location can be described using the Friedlander equation[10]:

$$P(t) = P_s[\exp(-t / t^*)] (1 - t / t^*) \quad (1)$$

where $P(t)$ is the time-dependent incident overpressure at a fixed distance from the explosion source, P_s is the peak shock overpressure at that distance, t is time, and t^* is the time duration (A-duration) that the pressure is above ambient (or the time at which the pressure makes the first zero-crossing).

For a 13-g spherical pentolite explosive charge (1:1 PETN($C_5H_8N_4O_{12}$): TNT($C_7H_5N_3O_6$)) detonated in air (above ground), at a standoff distance of 1.5 m from the pressure gauge, the explosive property calculator ConWep*[11] predicts the following:

Peak incident shock total pressure (P_s) = 124.615 kPa (23.3 kPa overpressure)

Positive phase duration (t^*) = 0.0008904 s

Figure 2 is a graph of Eq. 1 using the input parameters shown above for a 13-g spherical pentolite charge. The graph shows how the overpressure varies at a standoff distance of 1.5 m from the explosive center of mass (note that atmospheric pressure is ~101.325 kPa).

The Friedlander equation is often used to interpret pressure versus time records measured using blast gauges. For incident shock, the Friedlander curve is reasonably accurate in predicting the shape of the experimental pressure versus time record. For many applications, shock strength is reported as the positive area under

* Online access is limited to approved DOD users with a valid Common Access Card (CAC).

the pressure–time curve. The time from the initial pressure spike (P_s) to the first zero-pressure crossing (as referenced to ambient) is often referred to as the A-duration, with the area under this curve being the explosive impulse with units of Pa*s.[12]

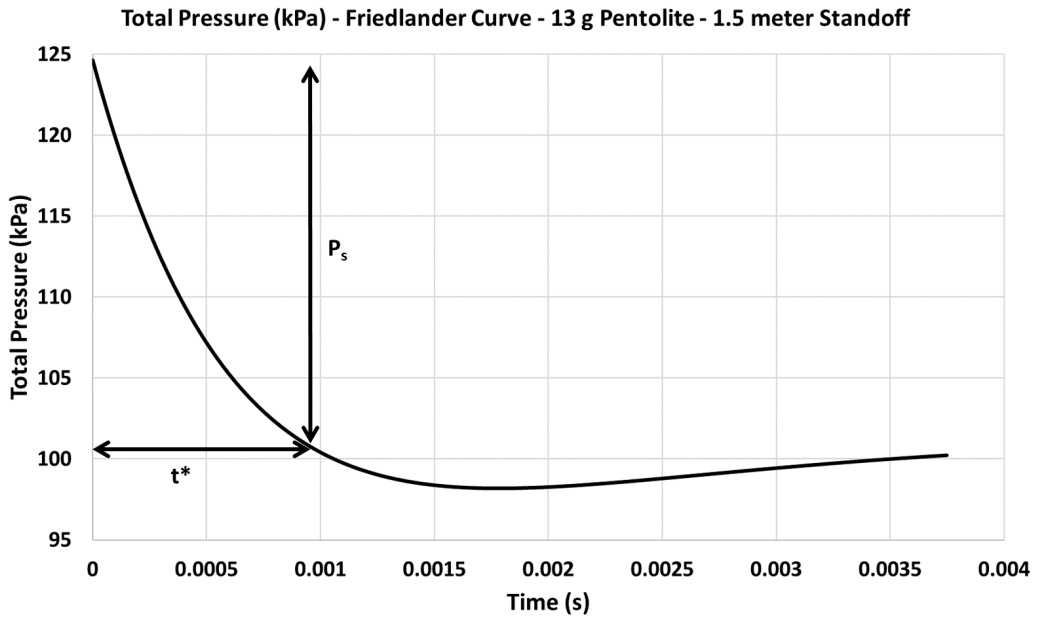

Fig. 2 A graph of Eq. 1 for a 13-g spherical pentolite charge. Pressure is calculated at a standoff distance of 1.5 m. Arrows indicate P_s (note that P_s is an overpressure; atmospheric pressure is 101.325 kPa) and t^* for this weight and standoff distance.

4. Theoretical Power of Detonation of a 13-g Pentolite Spherical Explosive at Standoff

The explosive pentolite is a 50:50 mixture of PETN and TNT, has a density of 1.65 g/cm^3, a detonation velocity near 7.4 km/s, and a detonation energy near 5.8 kJ/g. A 13-g sphere of pentolite will have a radius of 1.23 cm, with a detonation time (center detonation) near 1.66×10^{-6} s.[13]

The energy (J) of detonation of the 13-g sphere of pentolite is

$$E\ (J) = 13\ \text{g} * 5.8\ \text{kJ/g} = 75.4\ \text{kJ} \quad (2)$$

Figure 3 shows the energy (kJ) per square meter if the initial detonation energy is distributed over the surface of an expanding sphere. This is the maximum theoretical energy available per square meter at a distance from the exploding 13-g pentolite sphere. At a standoff of 1.5 m (a sphere with a radius of 1.5 m), the maximum amount of energy at the surface of the sphere is

$$75.4\ \text{kJ} / 28.27\ \text{m}^2 = 2.67\ \text{kJ/m}^2 \quad (3)$$

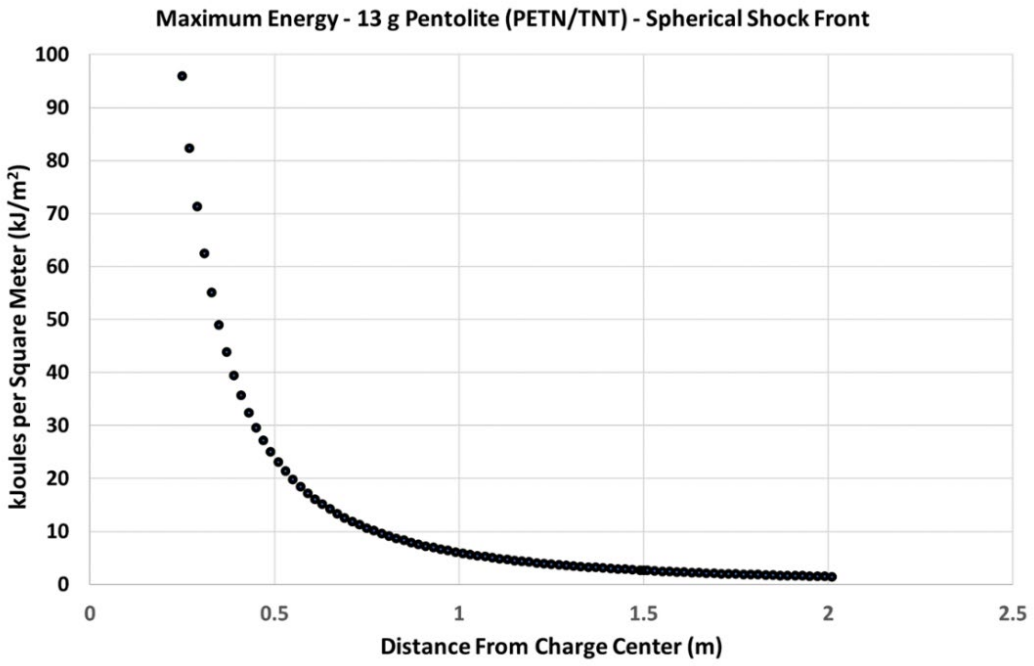

Fig. 3 The energy (kJ) available at the shock front (per square meter) assuming spherical expansion with no losses. This is the upper limit of energy available per square meter as a function of standoff for a 13-g exploding pentolite sphere.

If this energy is delivered in 0.89 ms (the measured A-duration at a 1.5-m standoff for 13 g of pentolite), the maximum power available per square meter is

$$2.67 \text{ kJ/m}^2 / 0.00089 \text{ s} = 3000 \text{ kW / m}^2 \quad (4)$$

If this power passes through a circular area 15 cm in diameter (approximately the diameter of the head of one of our test manikins[14]), the power through that area is

$$3.0 \text{ MW / m}^2 * 0.071 \text{ m}^2 = 213 \text{ kW} \quad (5)$$

This is the maximum power achievable for the 13-g pentolite charge at a standoff of 1.5 m through an area of 0.071 m^2, assuming no energy losses due to heat or light emission or from collisions with and between air molecules.

5. Shock Fluence Calculation Approach

We seek to calculate the energy in the airborne shock from data reported by a wearable blast gauge and compare this to the reported explosive impulse. The total kinetic energy of the envelope of shock-disturbed air moving in the direction of the shock is one-half the mass of air at a given velocity times that velocity squared, summed over the velocity distribution.[15] The average power of the envelope of shock-disturbed air is the total kinetic energy divided by the positive phase duration

(the A-duration). Figure 4 is a flowchart describing the process of calculating shock power from reported peak pressure and A-duration.

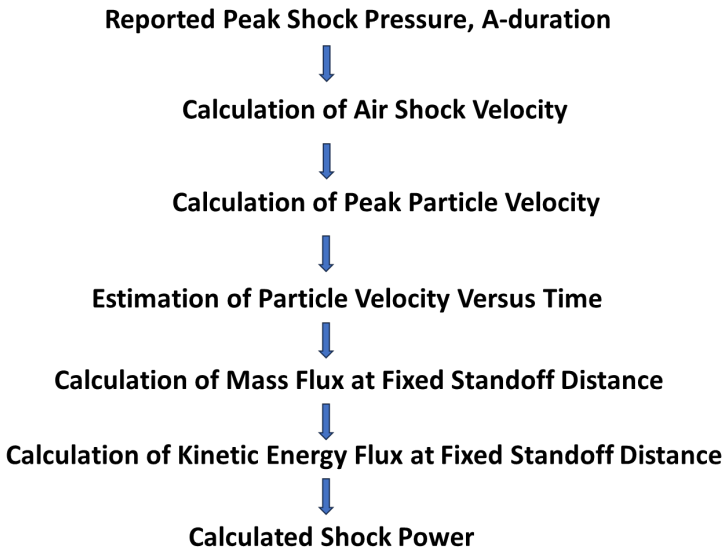

Fig. 4 A flowchart showing how power of a shock wave can be calculated from measured peak shock pressure and A-duration

6. Calculation of Air Shock Velocity

The peak pressure of an airborne shock wave (the pressure in the shock front, P_s in the Friedlander equation) is related to the velocity of shock wave propagation by the Rankine–Hugoniot equation[10]:

$$U = [c^2(1 + 6/7[P_s/P_0 - 1])]^{1/2} \quad (6)$$

where U is the shock front velocity, c is the sound speed in the ambient air, P_s is the peak incident shock absolute pressure, and P_0 is the absolute ambient pressure. Figure 5 is a graph of shock velocity versus peak shock incident overpressure. The arrow in Fig. 5 indicates the overpressure-shock velocity point for the 13-g pentolite charge at a standoff of 1.5 m. At a 1.5-m standoff, the predicted (Eq. 6) shock velocity produced by the 13-g pentolite explosive charge is 375.27 m/s.

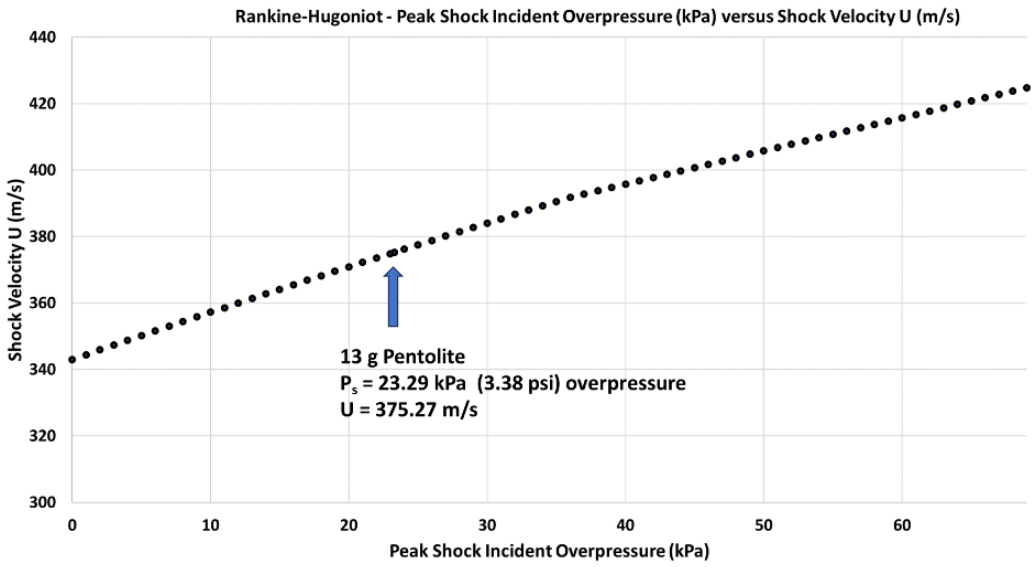

Fig. 5 A graph of shock velocity vs. peak shock incident overpressure using Eq. 6. The arrow in Fig. 5 indicates the overpressure–shock velocity point for the 13-g pentolite charge at a standoff of 1.5 m.

7. Calculation of Peak Particle Velocity: Approximation of the *U-u* Hugoniot for Air

The passage of the shock imparts a bulk velocity to the air in the direction of shock propagation, called the particle velocity u.[5] The particle velocity (u) – shock velocity (U) Hugoniot allows for calculation of peak particle velocity (u_p) when the shock front velocity (U) is known.[16]

Figure 6 is a graph of shock front velocity (U) versus peak particle velocity (u_p) for airborne shock. Data to construct this graph is from Deal[17] and ConWep.[11] A second-order polynomial fit to the data in Fig. 6 provides the following approximation to the u-U Hugoniot:

$$u_p = -2.433 \times 10^{-4} U^2 + 1.5845 U - 504 \qquad (7)$$

Using Eqs. 6 and 7 for the 13-g pentolite sphere at a standoff of 1.5 m,

$$u_p = 50.97 \text{ m/s}$$

It is worth noting that Eq. 7 is nonphysical—the polynomial just relates the numerical value of U to u_p. Both quantities have units of meters per second. The important aspect of Eqs. 6 and 7 is that peak particle velocity (u_p) can be calculated using measured peak shock pressure (P_s) for a given standoff distance. At this point we have an estimation of the peak particle velocity for the airborne shock (13-g pentolite) at a standoff of 1.5 m based only on the peak reported shock pressure.

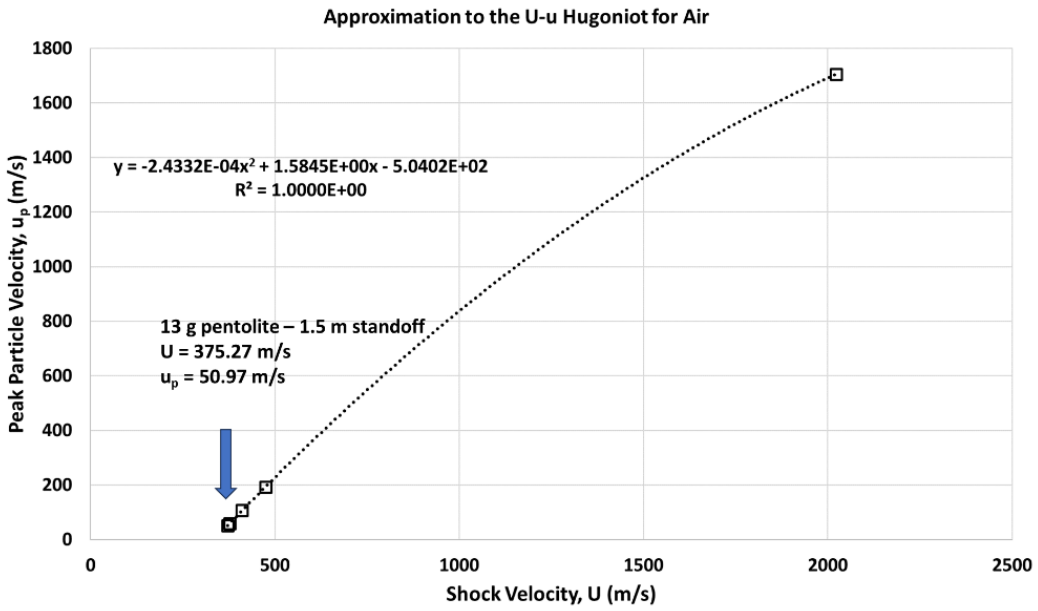

Fig. 6 A graph of shock velocity (U) vs. peak particle velocity (u_p) for airborne shock. Data used to construct this graph is from Deal[17] and ConWep.[11] The arrow indicates the U-u_p point for the 13-g pentolite charge at a standoff of 1.5 m.

8. Estimation of Particle Velocity vs. Time

To determine the energy of the shocked air molecules as they pass a standoff distance, it is necessary to calculate the particle velocity within the shock envelope. We estimate the particle velocity to be proportional to shock overpressure using a relationship suggested by Dewey, similar to the Friedlander equation[12]:

$$u(t) = u_p\,[\exp(-t / t^*)](1 - t / t^*) \tag{8}$$

where $u(t)$ is the time evolution of particle velocity at a fixed distance from the explosion source, u_p is the peak particle shock velocity (from Eq. 7), t is time, and t^* is the time duration (A-duration) of the shock with overpressure P_s. Figure 7 shows a graph of air particle velocity (u) versus time for an airborne shock produced by the detonation of 13 g of pentolite using Eq. 8. The standoff distance is 1.5 m. As expected, the particle velocity decreases to zero at time = t^*.

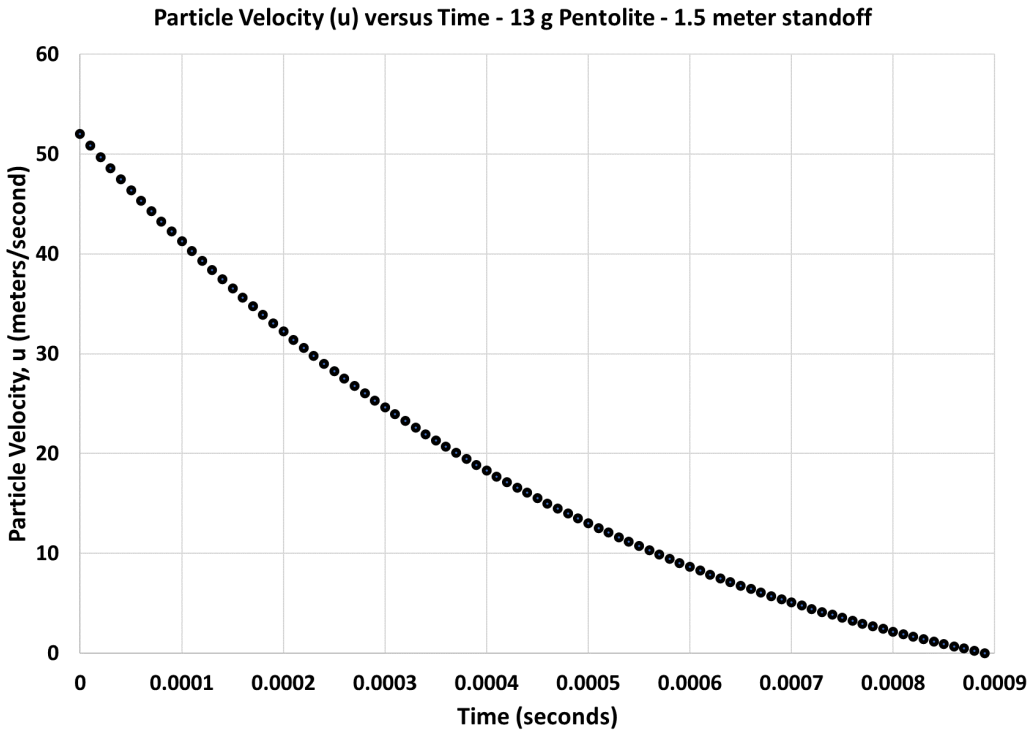

Fig. 7 A graph of particle velocity vs. time for an airborne shock produced by 13 g of pentolite. The standoff distance is 1.5 m. As expected, the particle velocity goes to zero as *t* approaches *t.**

9. Air Density

Calculating the kinetic energy of shock-disturbed gases requires an estimate of the mass of gas particles moving past the standoff distance. The density of dry air can be expressed as[18]

$$\rho = Pm / k_B T \tag{9}$$

where

ρ = density (kg/m^3), P = absolute pressure (Pa), m = molecular mass of dry air = 4.81×10^{-26} kg, k_B = Boltzmann's constant = 1.38×10^{-23} JK^{-1}, and T = temperature (K).

Equation 9 predicts the air density at the shock front (ρ_p) at a 1.5-m standoff for the 13-g pentolite charge to be 1.482 kg-m^{-3}.

10. Calculation of Mass Flux at Fixed Standoff Distance

The time dependence of the density of air as a shock passes a fixed standoff distance (ρ (t)) can be approximated using a form of the Friedlander equation[12]:

$$\rho\,(t) = \rho_p[\exp(-t / t^*)](1 - t / t^*) \quad (10)$$

Here, (ρ_p) is the air density at the shock front. The mass flux (mass(t)) is the rate at which mass flows through an imaginary surface at a given standoff distance from the explosive charge:

$$\text{mass}\,(t) = (\text{area}\ (\text{m}^2)) * (\text{density}\ (\text{kg/m}^3)) * (\text{velocity}\ (\text{m/s})) = A\,\rho(t)\,u(t) \quad (11)$$

Combining Eqs. 8, 10, and 11,

$$\text{mass}\,(t) = A\rho_p\,u_p[\exp(-2t / t^*)](1 - t / t^*)^2 \quad (12)$$

The units of Eq. 12 are kilograms per second (kg/s). Figure 8 shows the mass flux flowing through an area of 0.071 m^2 at 1.5-m standoff for a 13-g pentolite explosive charge as a function of time.

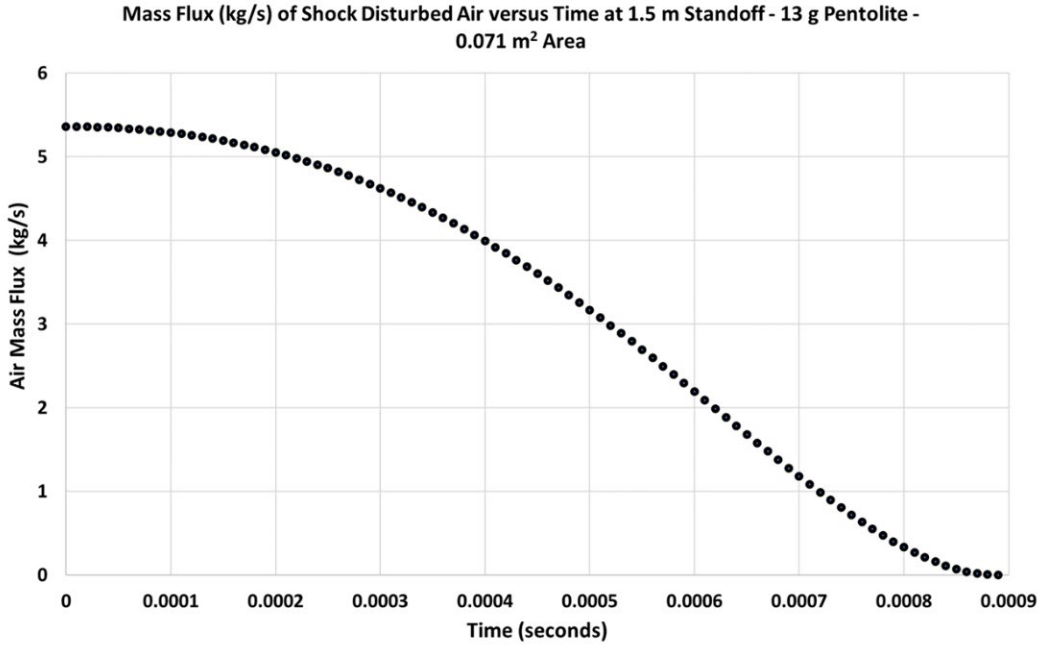

Fig. 8 Mass flux (kg/s) of shock disturbed air vs. time passing through an area of 0.071 m^2 at a standoff distance of 1.5 m from an exploding 13-g pentolite charge

11. Calculation of Kinetic Energy Flux at Fixed Standoff

The kinetic energy flux (J/s) of shock-disturbed air versus time (kinetic energy flux(t)) passing through an area of 0.071 m^2 at a standoff distance of 1.5 m from an exploding 13-g pentolite charge is one-half the product of the mass flux (Eq. 12) and the square of the particle velocity (Eq. 8):

$$\text{KE flux}(t) = [\text{mass}(t) * (\text{velocity}(t))^2]/2$$

$$\text{KE flux}(t) = (A\rho_p\,u_p\,[\exp(-2t / t^*)](1 - t / t^*)^2)\,[u(t)]^2/2 \quad (13)$$

$$\text{KE flux}(t) = (A\rho_p u_p^3[\exp(-4t / t^*)](1 - t / t^*)^4)/2 \qquad (14)$$

The units of Eq. 14 are joules per second (J/s). Figure 9 is a graph of kinetic energy flux (J/s) versus time and pressure versus time (Friedlander curve) for the air shock produced at a 1.5-m standoff by the exploding 13-g pentolite charge.

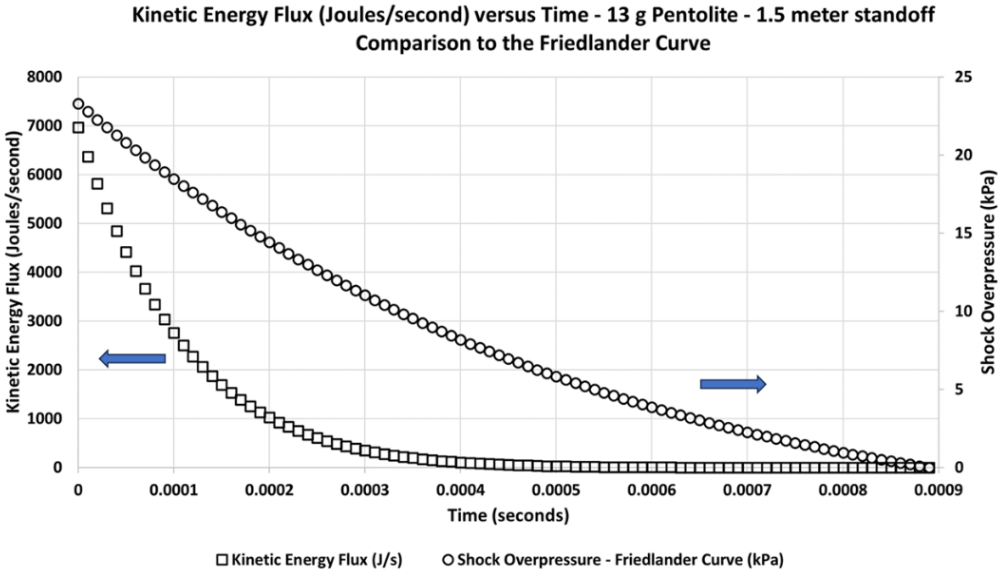

Fig. 9 The kinetic energy flux (J/s) passing through an area of 0.071 m^2 for airborne shock vs. time produced by 13 g of pentolite (Eq. 14). The standoff distance is 1.5 m.

The integral of the flux (the area under the kinetic energy flux curve in Fig. 9) is the fluence (total energy that passes through the 0.071 m^2 surface). A numerical integration of Eq. 14 gives a fluence at 1.5-m standoff through an area of 0.071 m^2 (15-cm-diameter circle) of 0.747 J. This energy is delivered in 0.00089 s (the A-duration) giving an average power of 0.839 kW. This is in comparison to Eq. 5, which predicted a maximum theoretical power at 1.5-m standoff of 213 kW for the 13-g pentolite explosive charge. This calculation suggests that the measured power delivered at 1.5-m standoff by the 13-g pentolite explosive charge is 0.39% of maximum theoretical power.

12. Power vs. Impulse

Figure 10 is a graph comparing explosive power on target (kW) at a 1.5-m standoff (0.071 m^2 area) with impulse (Pa*s) for pentolite explosive charges from 0.013 to 4.5 kg. Both quantities (power and impulse) are calculated using P_s and t^* values from ConWep.[11] Power values are calculated using an integration (from $t = 0$ to $t = t^*$) of Eq. 14. Impulse values are calculated using Dewey's analytical solution to the integral of the first positive phase of the Friedlander equation.[12] To a first approximation, both quantities increase with increasing explosive weight.

Explosive impulse tends to "level off" at higher explosive charge weights because the increase in shock velocity with explosive weight is eventually offset by decreasing the A-duration. The impulse is driven by shock pressure that, in turn, is a function of gas kinetic energy, and so the square of the particle velocity drives the initial increase in impulse with charge weight.

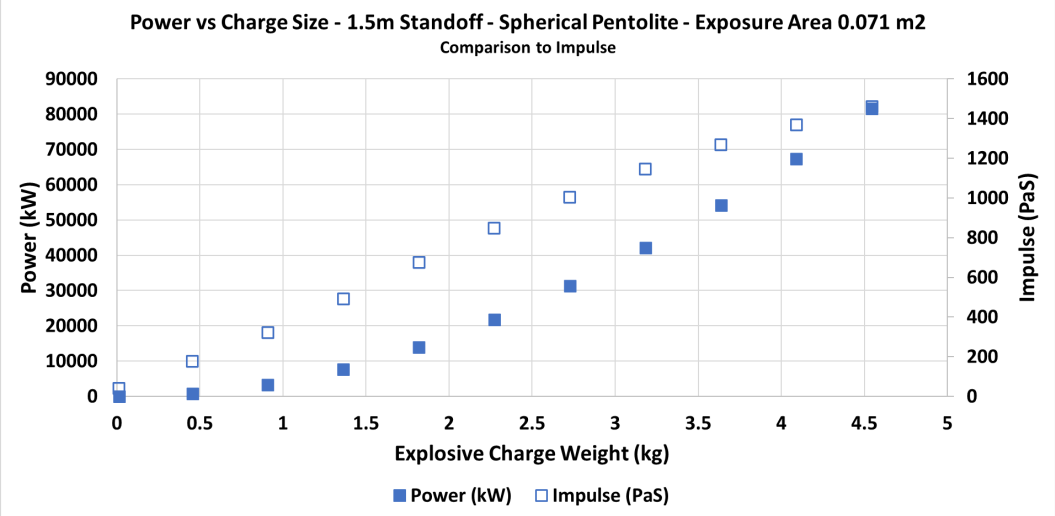

Fig. 10 A graph comparing power on target (kW) at 1.5-m standoff (0.71 m^2 area) with impulse (Pa*s) for pentolite explosive charges from 0.013 to 4.5 kg

The power has a slightly more exponential dependence on explosive charge mass because it has a cubic dependence upon particle velocity. The cubic dependence arises from the addition of a particle velocity component to the mass flux (see Eq. 12). This tends to compensate for the decrease in A-duration with charge size.

13. Discussion

For some wearable blast gauges,[19,20] pressure versus time data is fit to a Friedlander-type equation for which the variable fitting parameters are peak shock pressure (P_s) and positive phase duration (t^*). In the work presented here, power and impulse are calculated from these two parameters. We believe this approach is warranted but recognize it is inherently flawed because for some gauges with limited sampling bandwidth, P_s can be underreported, or affected by the surface to which the gauge is mounted. Additionally, variation in mounting surfaces (e.g., gauge mounted on a stick, gauge mounted on a wall, gauge mounted on personnel clothing) can affect t^* and the "shape" of the pressure–time curve from peak to first zero crossing. Perhaps most importantly, P_s is highly dependent on whether a shock is measured in reflected or incident configuration, or somewhere between those two limits. The purpose of this work is to propose an alternative way of interpreting P_s

and t^* values that expresses shock strength in units compatible with power measurement (W).

The average power of an airborne shock can be expressed in terms of the integral of the kinetic energy flux that flows through an imaginary surface divided by the A-duration. We have specified the surface as the cross-sectional area of the head of one of our test manikins (0.071 m^2). The surface is at a standoff distance defined by the user. We imagine the flux through this surface just prior to encountering any barrier or obstacle. In this way we have separated the problem of determining an object shock dose into two parts: the incident power of the incoming airborne shock wave and the effect of that shock wave on the target. The effect on target is not considered here. However, we believe the first part of determining the effect on target is to determine the angle between the surface experiencing the flux and the vector normal to the approaching shock surface (i.e., the degree to which the shock–target interaction is incident or reflective). Determining this angle is central to quantifying an object shock dose.

In the work presented here, there are at least three calculational difficulties that could benefit from further analysis. First, the change in particle velocity and density with time at a fixed standoff is assumed to vary with a Friedlander-type dependence. Dewey has proposed this,[12] but we are not aware of a justification in other parts of the literature. It does aid in making the expression for kinetic energy flux simple. Second, we have used a numerical integration method to determine the energy fluence (integral of Eq. 14). An analytical method is provided in the appendix of this report. Third, the approximation to the u-U Hugoniot for air could be more detailed.

From a qualitative viewpoint, we believe shock power to be a valuable complement to shock impulse. The reason is that the power has a cubic dependence upon particle velocity (because the particle velocity determines mass flux) while impulse is dependent on the square of the particle velocity. This increases the importance of higher-velocity air molecules in the shock with respect to the power calculation and provides a weighting to peak shock pressure not present in the calculation of shock impulse.

Additionally, we believe there is a slight advantage to reporting power on target in watts because this quantity can be directly related to the detonation energy of a given explosive. We think this may be a complement to efforts toward formulating/synthesizing energetic materials for downrange effect. Finally, by characterizing any airborne shock in terms of power, shocks from diverse sources (gun firings, chemical explosions, collisions, etc.) can be rated on a severity scale

traceable back to net explosive weight equivalency. We believe this may be a useful comparator to current methods of scaling explosive effects.

The appendix provides a step-by-step example of a calculation to determine the power of airborne shock from a pentolite charge at 164-g charge weight at a 1.5-m standoff.

14. Conclusion

This work provides an alternative method of scaling the strength of airborne shock by calculating shock power (watts) using only the peak measured shock pressure and duration of first positive pressure phase at a fixed standoff distance from the explosive source. We believe this work provides a complement to calculations of shock impulse based on the same input parameters. By approaching the power measurement as a kinetic energy flux calculation, the method described here weights peak pressure in a way not available for most impulse calculations.

15. References

1. Stoner G, Bleakney W. The attenuation of spherical shock waves in air. J Appl Phys. 1948;19,670–678.
2. Tovar MA, Bell RS, Neal CJ. Epidemiology of blast neurotrauma: a meta-analysis of blast injury patterns in the military and civilian populations. World Neurosurgery. 2021l;146:308–314.e3. doi: 10.1016/j.wneu.2020.11.093.
3. MacDonald CL, Johnson AM, Cooper D, Nelson EC, Werner NJ, Shimony JS, Snyder AZ, Raichle ME, Witherow JR, Fang R, et al. Detection of blast-related traumatic brain injury in US military personnel. New Eng J Med. 2011;364(22):2091–2100.
4. Committee on Gulf War and Health. Gulf War and Health. National Academies Press; 2014 Apr 14. (Long-term effects of blast exposures; vol. 9). Chapter 3, Pathophysiology of blast injury and overview of experimental data. https://www.ncbi.nlm.nih.gov/books/NBK202251.
5. Cooper P, editor. Explosives engineering. Wiley-VCH; 1996.
6. Kinney GF, Graham KJ. Explosive shocks in air. 2nd ed. Springer-Verlag; 1985.
7. Shin J, Whittaker AS, Cormie D. Incident and normally reflected overpressure and impulse for detonations of spherical high explosives in free air. J Struct Eng. 2015 Dec;141(12).
8. PCB Piezotronics, Inc. ICP© free-field blast pressure sensors; c2024 [accessed 2024 May 20]. https://www.pcb.com/sensors-for-test-measurement/pressure-transducers/blast-transducers/icp-free-field-blast.
9. Endeavor Business Media, LLC. Fundamentals of pressure transducers; c2024 [accessed 2024 May 28]. https://www.powermotiontech.com/home /whitepaper/21886841/fundamentals-of-pressure-transducers-pds-download.
10. Almustafa MK, Nehdi ML. Fundamental review on collision of blast waves. Phys Fluids. 2023;35(3). doi: 10.1063/5.0138156.
11. Army Corps of Engineers (US). Protective design center; last modified 10 June 2017 [accessed 2024 May 28]. https://intelshare.intelink.gov/sites/pdc/SitePages/Home.aspx.
12. Dewey JM. The Friedlander equations. In: Sochet I, editor. Blast effects. Shock wave and high pressure phenomena. Springer; 2018. doi: 10.1007/978-3-319-70831-7_3.

13. Kohler J, Meyer R. Explosives. 4th ed. VCH Publishers; 1993.

14. McNesby KL, Homan BE, Benjamin RA, Boyle VM, Densmore JM, Biss MM. Rev Sci Instrum. 2016;87:051301. doi: 10.1063/1.4949520.

15. Zhou X, Miao Y-R, Shaw WL, Suslick KS, Dlott DD. Shock wave energy absorption in metal–organic framework. J Am Chem Soc. 2019;141(6):2220–2223. doi: 10.1021/jacs.8b12905.

16. Mader CL. Numerical modeling of explosives and propellants. 3rd ed. CRC Press; 2008.

17. Deal WE. Shock Hugoniot of air. J Appl Phys. 1957;28(7):782–784.

18. Alberty RA, Daniels F. Physical chemistry. 5th ed. John Wiley and Sons; 1979.

19. BlackBox Biometrics; c2022 [accessed 2024 May 29]. https://b3inc.com/.

20. Med-Eng; c2024 [accessed 2024 May 29]. https://www.med-eng.com/.

Appendix. Example Calculations

A.1 Calculating Power on Target from Blast Gauge Data

Using reported blast gauge data to calculate power on target at a given standoff distance via the methods outlined here assumes a "Friedlander-type" shape of the pressure versus time record. To calculate power on target requires measured t^* values and conversion of measured P_s values to peak particle velocity and peak air density. Also required are measurements of ambient pressure and temperature. With these quantities in hand, Eqs. A-1 and A-2 are used to calculate peak particle velocity (u_p), and Eq. A-3 is used to calculate peak air density (ρ_p) at the shock front.[1]

$$U = [c^2(1 + 6/7[P_s / P_0 - 1])]^{1/2} \quad \text{(A-1)}$$

where U is the shock front velocity, c is the sound speed in the ambient air, P_s is the peak incident shock absolute pressure, and P_0 is the absolute ambient pressure.

The particle velocity (u) – shock velocity (U) Hugoniot (Eq. A-2) allows for calculation of peak particle velocity (u_p) when the shock front velocity (U) is known[2]:

$$u_p = -2.433 \times 10^{-4}\, U^2 + 1.5845U - 504 \quad \text{(A-2)}$$

The density of air in the shock front is approximated as[3]

$$\rho = Pm / k_B T \quad \text{(A-3)}$$

where ρ = density (kg/m^3), P = absolute pressure (Pa), m = molecular mass of dry air = 4.81×10^{-26} kg, k_B = Boltzmann's constant = 1.38×10^{-23} JK^{-1}, and T = temperature (K). The kinetic energy flux is given by Eq. A-4, incorporating values from A-1, A-2, and A-3:

$$\text{KE flux}(t) = (A\rho_p\, u_p^3[\exp(-4t / t^*)](1 - t / t^*)^4)/2 \quad \text{(A-4)}$$

The steps to determine the KE flux are as follows:

1) Determine sound speed (c in Eq. A-1) at ambient conditions (from lookup table[4]).

2) Determine atmospheric pressure (P_0) at ambient conditions (measured).

---

[1] Almustafa MK, Nehdi ML. Fundamental review on collision of blast waves. Phys Fluids. 2023;35(3). doi: 10.1063/5.0138156.

[2] Mader CL. Numerical modeling of explosives and propellants. 3rd ed. CRC Press; 2008.

[3] Alberty RA, Daniels F. Physical chemistry. 5th ed. John Wiley and Sons; 1979.

[4] Speed of sound vs. elevation, temperature, and air pressure. The Engineering ToolBox; 2009 [accessed 2024 May 28]. https://www.engineeringtoolbox.com/elevation-speed-sound-air-d_1534.html.

3) Calculate ρ_p using P_s in Eq. A-3.

4) Calculate U from Eq. A-1 and P_s.

5) Calculate u_p from U using Eq. A-2.

6) Numerically integrate the following:

   Kinetic energy flux(t) = $(A\rho_p u_p^3[\exp(-4t / t^*)(1 - t / t^*)^4])/2$

   from $t = 0$ to $t = t^*$.

   (This is fluence [total energy (J)] on target at the standoff distance.)

7) Divide the result of Step 6 by t^*.

   (This is power on target – fluence/A-duration – W.)

Example Calculation

For a 164-g pentolite charge measured after explosion at a 1.5-m standoff, the input variables are

$A = 0.071$ m^2

$T = 293$ K (measured)

$c = 343$ ms^{-1} (from lookup table[4])

$P_0 = 101325$ Pa (measured)

$P_s = 213.825$ (measured by gauge)

$t^* = 1.41 \times 10^{-3}$ s (measured by gauge)

Calculate ρ_p using P_s in Eq. A-3:

$\rho = Pm / k_B T$

$\rho = 2.544$ kg/m^3

Calculate U from Eq. A-1 and P_s:

$U = [c^2(1 + 6/7[P_s/P_0 - 1])]^{1/2}$

$U = 479.18$ m/s

Calculate u_p from U using Eq. A-2:

$u_p = -2.433 \times 10^{-4} U^2 + 1.5845U - 504$

$u_p = 199.2$ m/s

Plot kinetic energy flux versus time from $t = 0$ to $t = t^*$:

$$\text{KE flux}(t) = (A\rho_p u_p^3[\exp(-4t / t^*)(1 - t / t^*)^4])/2 \qquad \text{(A-4)}$$

Integrate Eq. A-4 from time = 0 to time = t^*. This is fluence (J).

Figure A-1 plots kinetic energy flux (J/s) versus time for an exploding 164-g pentolite charge. (We do this numerically; an analytical solution to the integral in Eq. A-5 is provided in Section A.2 here.)

$$\text{KE fluence} = \int(A\rho_0 u_0^3[\exp(-4t / t^*)(1 - t / t^*)4])/2 \, dt \qquad \text{(A-5)}$$

Kinetic energy fluence (J) = 121 J

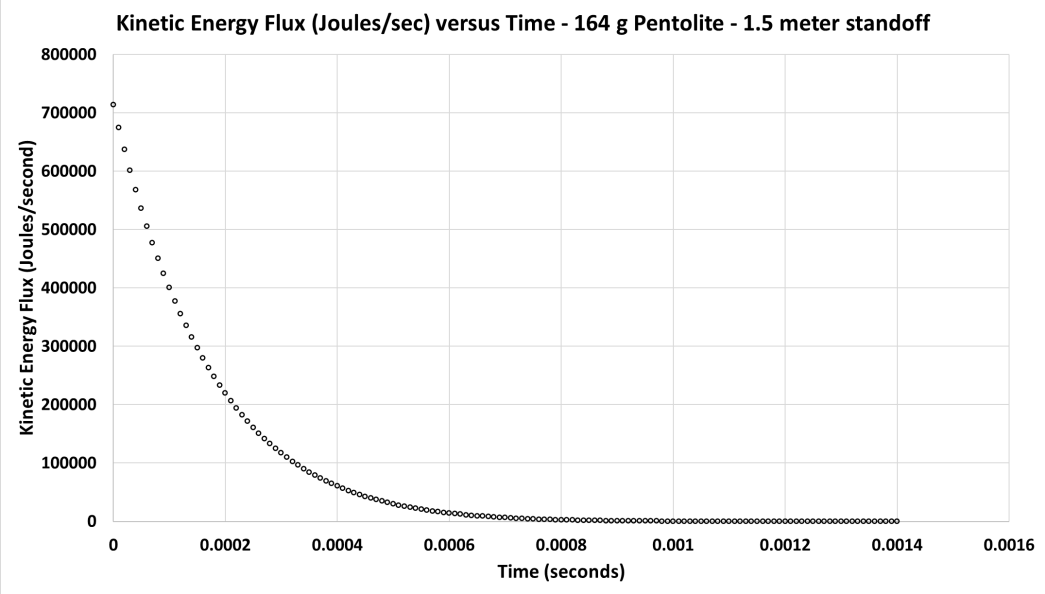

Fig. A-1 A plot of kinetic energy flux (J/s) vs. time (Eq. A-4) for an exploding 164-g pentolite charge

Divide kinetic energy fluence by t^* to get power.

Power (W) = kinetic energy fluence / t^*

Power (W) = 85.83 kW

A calculation of maximum theoretical power (see Section 4 of main report) yields a value of 1694.2 kW. For this charge size, approximately 5.1% of maximum theoretical power of the 164-g pentolite charge is delivered on target for a 1.5-m standoff.

This value is higher than that for the 13-g pentolite charge because a main loss of shock energy is from successive air collisions that propagate the air shock. For larger charge sizes, the distance travelled through air decreases relative to smaller

charge sizes (for a fixed standoff) because the amplitude of travel of the "piston" launching the air shock increases.

A.2 Analytical Solution of the Fluence Integral

An analytical solution to the time integral of Eq. A-4 is provided in Eq. A-6:

$$\int \text{KE flux}(t)dt \; = A\,\rho_0\,{u_0}^3\,e^{-4t/t^*}\left(-\frac{t^4}{8t^{*3}}+\frac{3t^3}{8t^{*2}}-\frac{15t^2}{32t^*}+\frac{17t}{64}-\frac{15t^*}{256}\right)+C \qquad \text{(A-6)}$$

Evaluating the integral for the 13-g spherical pentolite charge from $t = 0$ to $t = t^*$ results in 0.7311 J of kinetic energy during the A-duration.

$$E=\int_0^{0.00089}\frac{1}{2}(0.071m^2)(1.496kg/m^3)(50.97m/s)^3 e^{\frac{-4t}{(0.000809s)}}\left(1-\frac{t}{(0.000809s)}\right)^4 dt = 0.7311J \qquad \text{(A-7)}$$

Dividing this energy by t^* gives an average power of 0.821 kW delivered to the manikin's head during the A-phase at a standoff of 1.5 m for the 13-g pentolite charge, slightly less than the power predicted by the numerical integration of Eq. A-4 (0.839 kW).

List of Symbols, Abbreviations, and Acronyms

KE	kinetic energy
PETN	pentaerythritol tetranitrate
TNT	trinitrotoluene